Pathogen lifestyle defines host genetic signature of quantitative disease resistance in oilseed rape (*Brassica napus)*

Catherine N. Jacott[1], Henk-jan Schoonbeek[1], Burkhard Steuernagel[2], Rachel Kirby[1], Xiaorong Zheng[3], Andreas von Tiedermann[3], Violetta K. Macioszek[4], Andrzej K. Kononowicz[5], Heather Fell[6], Bruce D.L. Fitt[6], Georgia K. Mitrousia[6,7], Henrik U Stotz[6], Christopher J. Ridout[1], Rachel Wells[1].

[1] Crop Genetics Department, John Innes Centre, Norwich Research Park, Norwich, NR4 7UH, UK

[2] Computational and Systems Biology Department, John Innes Centre, Norwich Research Park, Norwich, NR4 7UH, UK

[3] Department of Crop Sciences, Georg August University, Göttingen, Germany

[4] Department of Biology and Plant Ecology, Faculty of Biology, University of Bialystok, 15-245 Bialystok, Poland

[5] Department of Plant Ecophysiology, Faculty of Biology and Environmental Protection, University of Lodz, 90-237 Lodz, Poland

[6] Centre for Agriculture, Food and Environmental Management Research, School of Life and Medical Sciences, University of Hertfordshire, Hatfield, Hertfordshire AL10 9AB, UK

[7] Rothamsted Research, Harpenden, Hertfordshire, AL5 2JQ, UK

Authors for correspondence: Rachel Wells

Email: rachel.wells@jic.ac.uk

ORCiDs

Catherine N. Jacott	http://orcid.org/0000-0002-4285-0228
Henk-jan Schoonbeek	http://orcid.org/0000-0002-1087-2553
Burkhard Steuernagel	http://orcid.org/0000-0002-8284-7728
Rachel Kirby	NA
Xiaorong Zheng	http://orcid.org/0000-0002-1369-8669
Andreas von Tiedermann	http://orcid.org/0000-0002-1085-9607
Violetta K. Macioszek	http://orcid.org/0000-0002-5143-4226
Andrzej K. Kononowicz	http://orcid.org/0000-0001-9950-5102
Heather Fell	NA
Bruce D.L. Fitt	http://orcid.org/0000-0003-3981-6456
Georgia K. Mitrousia	http://orcid.org/0000-0002-5960-6555
Henrik U Stotz	http://orcid.org/0000-0003-2954-8566
Christopher J. Ridout	http://orcid.org/0000-0001-9287-938X
Rachel Wells	http://orcid.org/0000-0002-1280-7472

Total word count: 6457 words

Summary: 179 words

Introduction: 1093 words

Materials and Methods: 1173 words

Results: 2616 words, 6 tables, 4 figures (colour), 7 supporting tables, 2 supporting figures (colour)

Discussion: 1575 words

Summary

- Crops are affected by several pathogens, but these are rarely studied in parallel to identify common and unique genetic factors controlling diseases. Broad-spectrum quantitative disease resistance (QDR) is desirable for crop breeding as it confers resistance to several pathogen species.
- Here, we use association transcriptomics (AT) to identify candidate gene loci associated with *Brassica napus* QDR to four contrasting fungal pathogens: *Alternaria brassicicola*, *Botrytis cinerea*, *Pyrenopezia brassicae* and *Verticillium longisporum.*
- We observed broad-spectrum QDR dependent on the lifestyle of the fungal pathogen—hemibiotrophic and necrotrophic pathogens had distinct QDR responses and associated loci—suggesting potential trade-offs associated with such molecular determinants. We observed some loci involved in both early immune signalling and downstream QDR. In addition, we identify a novel QDR locus associated with resistance to *V. longisporum*.
- This is the first time AT has been used simultaneously for several pathosystems to identify loci involved in broad-spectrum QDR. As interesting candidates for crop breeding, we specifically highlight candidate loci for broad-spectrum QDR—to either the hemibiotrophic or necrotrophic pathogens—with no antagonistic effects on susceptibility to other pathogens.

Key words

association transcriptomics, *Brassica napus,* broad-spectrum resistance, PAMP-triggered immunity, quantitative disease resistance

Introduction

Crop-infecting fungi are responsible for approximately 20% of global crop losses annually (Fisher *et al.*, 2018). Broad-spectrum resistance is desirable for controlling crop disease because it protects against several pathogen species or most races or isolates of the same pathogen (Kou and Wang, 2010). Despite this, plant interactions with different pathogens are rarely studied in parallel to identify common and unique genetic factors controlling the diseases.

Most breeding efforts focus on *'R'* (resistance) gene-mediated qualitative resistance, often providing complete resistance to only some races of a specific pathogen (McDowell and Woffenden, 2003). *R* gene-mediated resistance is often short-lived and breaks down when pathogen effector genes mutate. In contrast, quantitative disease resistance (QDR) presents a continuous distribution of phenotypes from susceptible to resistant and has great potential for crop breeding since it is often broad-spectrum and durable. However, QDR is not routinely selected in breeding programs because genetic information on the underlying molecular determinants is lacking (Roux *et al.*, 2014; Nelson *et al.*, 2018).

Broad-spectrum resistance conferred by QDR genes could relate to the pathogen perception and initial signalling response pathways of pathogen-associated molecular pattern (PAMP)-triggered immunity (PTI), effector-triggered defence (ETD) or effector-triggered immunity (ETI) (Roux *et al.*, 2014). PAMPs are recognised by cell surface-localized pattern-recognition receptors (PRRs). Upon PAMP recognition, plants rapidly produce reactive oxygen species (ROS) like H_2O_2, followed by mitogen-activated protein kinase (MAPK) activation and induction of defence genes. Different PAMPs—such as chitin from fungal cell walls, flg22 from bacterial flagellin, and elf18 from bacterial Elongation factor-Tu (EF-Tu)—require distinct PRRs for their recognition, but there are common downstream components after PRR-PAMP recognition including Respiratory Burst Oxidase Homologue D (RBOHD) which is required to produce H_2O_2 (Gómez-Gómez and Boller, 2000; Kunze *et al.*, 2004; Miya *et al.*, 2007; Sang and Macho, 2017). Like QDR, PTI is broad spectrum and is the key factor in non-host (complete) resistance, whereby most plants are resistant to most microbial pathogens (Nelson *et al.*, 2018). To facilitate invasion,

adapted pathogens deliver effectors into the plant apoplast or cytoplasm to suppress host immunity. Upon recognition of effectors, plants activate more powerful immune responses, effector-triggered defence (ETD) for apoplastic pathogens (Stotz *et al.*, 2014) and effector-triggered immunity (ETI) for intracellular pathogens. Both ETD and ETI often result in host cell death to restrict pathogen invasion.

Some quantitative trait loci identified for QDR resemble PRRs or receptor-like kinases like those involved in PTI, ETD or ETI (Wisser *et al.*, 2005; Schweizer and Stein, 2011; Hurni *et al.*, 2015; Nelson *et al.*, 2018). Interestingly, the strength of flg22 perception is positively correlated with resistance to *Pseudomonas syringae* in Arabidopsis (*Arabidopsis thaliana*) (Vetter *et al.*, 2012) but negatively correlated with resistance to Target Leaf Spot (*Bipolaris cookie*) in sorghum (*Sorghum bicolor*) (Samira *et al.*, 2020). Furthermore, disruption of the EF-Tu receptor (EFR) in *A. thaliana* increases susceptibility to bacterial pathogens and over-expression of EFR increases resistance to various bacterial pathogens in wheat, rice and tomato (Kunze *et al.*, 2004; Lacombe *et al.*, 2010; Schoonbeek *et al.*, 2015; Schwessinger *et al.*, 2015; Boschi *et al.*, 2017).

Broad-spectrum QDR responses may also relate to downstream immune outputs at the intersection between PTI, ETD and ETI (Roux *et al.*, 2014). Although PTI, ETD and ETI involve distinct receptors, activation mechanisms and early signalling components, they eventually converge into similar downstream responses (Yuan *et al.*, 2021). For example, PTI-induced ROS production and accumulation can lead to programmed cell death via MAPK cascades (Levine *et al.*, 1994; Jones, 2000; Kotchoni and Gachomo, 2006). Additional reported QDR mechanisms include enhanced cell wall synthesis (Wisser *et al.*, 2005; Corwin *et al.*, 2016), enhanced secondary metabolism (Benson *et al.*, 2015) and modified transport processes (Moore *et al.*, 2015; Deppe *et al.*, 2018). On the other hand, recent systems biology approaches suggest that key functions of QDR are distinct from those previously identified for plant immunity (Delplace *et al.*, 2020).

Plant pathogens are often referred to as biotrophic, hemibiotrophic, or necrotrophic, depending on their infection and feeding strategies. These strategies include feeding on living host cells (biotrophy); killing plant cells to feed on their contents (necrotrophy); and keeping cells alive while establishing infection before switching to a necrotrophic lifestyle (hemibiotrophy) (Kemen and Jones, 2012). Plants must accurately detect and appropriately respond to these different lifestyles, which is important to consider when breeding for broad-spectrum QDR (Corwin and Kliebenstein, 2017). For biotrophic and hemibiotrophic pathogens, the regulation of cell death through plant immune components like ETD/ETI-induced cell death or pathogen-induced ROS can provide effective resistance (Jia *et al.*, 2000; Vleeshouwers *et al.*, 2000). However, basal defences like cell death are often not effective against necrotrophic pathogens (Laluk and Mengiste, 2010) because necrosis can condition susceptibility and facilitate their colonization (Lorang *et al.,* 2007; Faris and Friesen, 2020). Similarly, pathogen-derived or pathogen-induced ROS accumulation can promote cell death and pathogenicity for some necrotrophs (Tiedemann, 1997; Williams *et al.*, 2011).

Oilseed rape (*Brassica napus*) is a major crop worldwide, producing edible oil, biodiesel and protein for animal feed. Diseases are a key factor affecting OSR production and improved resistance is a major target in breeding. We previously used associative transcriptomics (AT) (Harper *et al.*, 2012; Havlickova *et al.*, 2018) to identify candidate gene loci as single nucleotide polymorphisms (SNPs) and gene expression markers (GEMs) associated with *B. napus* QDR to *Pyrenopeziza brassicae* (Fell *et al.*, 2022). Other studies have used similar association genetics approaches to identify candidate resistance genes in *B. napus* (Dakouri *et al.*, 2021; Roy *et al.*, 2021) demonstrating the potential of AT for the identification of resistance loci for different pathosystems. However, to our knowledge, AT has never been used to research the similarities and differences between the loci underlying resistance to multiple pathogens.

In this study, we used AT to identify novel loci involved in QDR in *B. napus* using a common panel of *B. napus* genotypes. We focused on four contrasting fungal pathogens of *B. napus:* necrotrophic pathogens *Alternaria brassicicola* and *Botrytis cinerea,* and hemibiotrophic pathogens *P. brassicae,* and

Verticillium longisporum. For the first time, we demonstrate that AT analyses from several pathogens can be combined to identify candidate loci for broad-spectrum QDR. We identify GEMs associated with QDR to multiple pathogens and GEMs associated with either resistance or susceptibility dependent on the pathogen lifestyle. We also identify some GEMs associated with both PTI and QDR. Furthermore, we identify a potential deletion containing five candidate genes associated with resistance to *V. longisporum.* This study provides new insight into the commonalities underlying broad-spectrum QDR and provides a resource for improving broad-spectrum resistance to pathogens in *B. napus.*

Materials and Methods

Pathogen infection assays

Alternaria brassiciciola

151 available *B. napus* accessions were grown in peat soil (pH 5.6 – 6.8) with 1/30 by volume of Perlite, 16 h day/8 h night photoperiod under fluorescent light (Super TLD Philips 865, 100 µmol m^{-2} s^{-1}), 19°C ± 2°C and relative humidity of approximately 70%. The wild-type strain of *A. brassicicola* (ATCC 96836) was cultured and grown as described previously (Macioszek *et al.,* 2018). Conidial suspension prepared in distilled water was diluted to a final concentration of $3.5x10^5$ conidia ml^{-1}. The third leaf of five weeks old plants was inoculated with two 10 µl drops of conidial suspension. The necrotic area of three replicates per genotype was measured at 5 days post-inoculation (dpi) using WinDIAS_3 Imaging Analysis System (Delta-T Devices, UK). The experiment was repeated twice.

Botrytis cinerea

190 available *B. napus* accessions were divided into four groups for screening. Plants were grown in Levington F2 compost with 15% 4mm grit in growth chambers for 6-7 weeks under TL-tubes with a near-sunlight spectrum of 100 µmol m^{-2} s^{-1} with a photoperiod of 10 h. Temperatures were 20-22 °C/18-20 °C day/night. *Botrytis cinerea* strain B05.10 (Schoonbeek *et al.,* 2001) was grown

as described previously (Stefanato *et al.*, 2009) and used for inoculations as described (Lloyd *et al.*, 2014). Spore suspensions (200 µl at 2.5×10^6 spores ml^{-1}) were spread on 1/10 PDA (2.5 g l^{-1} potato dextrose broth, 12 g l^{-1} agar), grown for 24 h at 21°C and 4mm agar plugs were used for *B. napus* inoculations of 22 mm leaf discs on 0.6% water agar. The lesion diameter of 16 replicates per genotype was measured after 48 h at 21 °C with a relative humidity of 85-100% and low light levels (10-20 µmol m^{-2} s^{-1}). Two full experimental repeats were done.

Pyrenopeziza brassicae

The *P. brassicae* methods and phenotype dataset used were the same as in our previous publication (Fell *et al.*, 2022). Disease severity was scored on a scale of 1 to 6—with a score of 1 for no sporulation and 6 for the most sporulation—and was calculated for each of the 129 available genotypes.

Verticillium longisporum

191 available *B. napus* accessions were divided into four groups for screening. Six reference lines covering the range of resistance phenotypes were used for normalization: Falcon, SEM, Zhongyou, Loras (Georg August University Göttingen collection), Falcon and Loras (John Innes Centre collection). Each line had 20 plants for both mock and *V. longisporum* inoculation. The preparation of fungal inoculum and disease assessment was done as described previously (Zheng, 2018; Zheng *et al.,* 2019). Ten-day-old conidial suspension of *V. longisporum* isolate VL43 obtained from a diseased *B. napus* plant (Zeise and Tiedemann, 2001) was used for inoculation. Ten-day-old plants with cotyledons completely unfolded were washed from quartz sand and inoculated with water or $1x10^6$ CFU ml^{-1} spore suspension for 50 min. Plants were kept in a climate chamber with a 16 h photoperiod and a temperature of 22 ± 2 □C. Disease severity on stems ranging from 1 (healthy) to 9 (death) was assessed at 7, 14, 21, and 28 days after inoculation. The area under the disease progress

curve of all accessions was calculated from the disease severity scoring and normalized based on the internal reference lines.

ROS assays

190 available *B. napus* accessions were divided into four batches and grown in Levington F2 compost with 15% 4 mm grit in growth chambers for 5-6 weeks under TL-tubes with a near-sunlight spectrum at circa 100 µmol m^{-2} s^{-1} with a photoperiod of 10 h. Temperatures were 20-22°C/18-20°C day/night. ROS measurements were done with a luminol/peroxidase-based assay. For each accession, two leaf discs (4 mm diameter) were cut with a biopsy puncher (Miltex; www.integralife.com) from the second most recently expanded leaf of four individual plants and incubated in 200 µl sterile water in a 96-well plate for 16 to 24 h in the dark. The water was drained and replaced by a solution containing 34 mg l^{-1} luminol, 20 mg l^{-1} horseradish peroxidase (HRP) and PAMP: either chitin (100 g l^{-1}, NA-COS-Y, Yaizu Suisankagaku Industry CO, YSK, Yaizu, Japan); flg22 (QRLSTGSRINSAKDDAAGLQIA) or elf18 (SKEKFERTKPHVNVGTIG, both 10mM, Peptron, http://www.peptron.co.kr). Luminescence was recorded every 30 s over 40 min using a Varioskan Flash plate reader (www.fishersci.co.uk) and displayed as the sum of photon counts over this period. To calculate the dynamics of the ROS response we transformed the measurements into smoothed curves using the average of five adjacent measurements in a sliding window over all 80 time points. The area under the curve (total ROS response in arbitrary units) of each genotype was calculated. Two repeat experiments were done.

Phenotypic data transformation for association analysis

Each dataset (infection phenotypes for *A. brassicicola, B. cinerea, P. brassicae* or *V. longisporum,* ROS measurements for chitin, flg22 or elf18) was analysed using a linear fixed- and random effects model with *B. napus* genotype as a fixed effect and experimental replicate and batch as random effects. Estimated marginal means were calculated for each *B. napus* genotype using emmeans

(version 1.8.0) (R package). These data were used for input into the AT pipeline. For combined data visualization, the estimated marginal means were transformed into a range between 0 and 1. For pathogen datasets, the inverse of these values was used to represent 'resistance'.

Association transcriptomics

Genotype (SNP) and expression level datasets (Havlickova *et al.*, 2018), available from York Knowledgebase (http://yorknowledgebase.info) were used and reduced to include only the lines used within this study. Genome-Wide Association (GWA) and GEM mapping were done using the R-based GAGA pipeline (Nichols, 2022), which utilises GAPIT Version 3 (Lipka *et al.*, 2012; Wang and Zhang, 2021). GAGA was run using our recently updated population structure (Fell *et al.*, 2022) and *B. napus* Pantranscriptome version 11 (Havlickova *et al.*, 2018). GWA analyses were done using a generalised linear model (GLM); Bayesian-information and Linkage-disequilibrium Iteratively Nested Keyway (BLINK) (Huang *et al.*, 2019), and Fixed and random model Circulating Probability Unification (FarmCPU) (Liu *et al.*, 2016) to determine the optimal model. The best-fitting model was selected for final analysis by comparing QQ plots.

GEM associations were determined by linear regression using Reads Per Kilobase of the transcript, per Million mapped reads (RPKM) to predict a quantitative outcome of the trait value. All markers with an average expression of less than 0.5 RPKM were removed before analysis. The Pearson method was used to determine the correlation coefficient between expression and resistance phenotype for each GEM. The false discovery rates (FDR) for both GEM and GWA were determined using the Shiny implementation of the q-value R package (Storey, 2011).

The level of linkage disequilibrium (LD) varies between and across chromosomes depending on the position and level of selection. To determine the specific level of LD at the A09 locus identified for *V. longisporum* resistance,

we calculated the mean pair-wise R^2 for this marker compared to all markers on the chromosome using TASSEL Version 5.0 using the site by all analysis options (Bradbury *et al.*, 2007). Markers were considered in LD when $R^2 > 0.2$.

Results

QDR to *A. brassicicola, B. cinerea, P. brassicae* and *V. longisporum* is present in the *B. napus* population

We hypothesised that QDR to *A. brassicicola, B. cinerea, P. brassicae* and *V. longisporum* would be present in our *B. napus* population. We did pathogenicity assays on the *B. napus* genotypes and monitored susceptibility using the established methods for each pathosystem: necrotic area on leaves (*A. brassicicola* and *B. cinerea*), percentage leaf area with sporulation (*P. brassicae*) and area under disease progress curve for infection of stems (*V. longisporum*). The *B. napus* genotypes demonstrated varying levels of resistance to the pathogens suggesting that QDR was present in the population (Fig. **1**, Table **S1**).

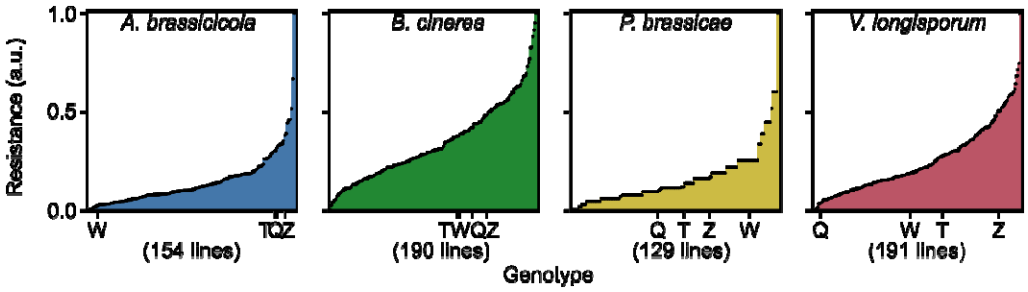

Fig. 1 *Brassica napus* disease resistance to fungal pathogens is quantitative. Resistance phenotype (arbitrary units (a.u.), normalized values between zero and one) of different *B. napus* genotypes to *Alternaria brassicicola*, *Botrytis cinerea*, *Pyrenopeziza brassicae* or *Verticillium longisporum.* The total number of genotypes used for each pathogen assay and the position of reference genotypes Quinta (Q), Tapidor (T), Westar (W) and Zhongshuang 11 (Z) are indicated.

To identify QDR loci, we did GWA analysis on our datasets. However, we did not identify any significant marker associations with resistance to any of the pathogens, using a false discovery rate of 0.05 (Table **S2**). We did GEM analyses using the transcriptomes of the *B. napus* genotypes to analyse resistance as a function of the expression of all gene models (Table **S3**). Numerous GEMs were significantly associated with resistance to fungal

pathogens (FDR < 0.05): 2129 GEMs for *A. brassicicola;* 370 GEMs for *B. cinerea;* 659 GEMs for *P. brassicae;* and 3222 GEMS for *V. longisporum.* We determined if the expression of the GEMs was positively or negatively correlated with the resistance phenotype and named these 'resistance GEMs' or 'susceptibility GEMs', respectively (Table **1**).

Table 1. The number of gene expression markers (GEMs) associated with resistance to *Brassica napus* fungal pathogens *Alternaria brassicicola, Botrytis cinerea, Pyrenopeziza brassicae and Verticillium longisporum.* The total numbers of GEMs, GEMs with expression positively correlated with resistance (R, resistance) and negatively correlated with resistance (S, susceptibility) are indicated.

	Number of GEMs (FDR < 0.05)		
Pathogen	**Total**	R	S
A. brassicicola	2129	627	1502
B. cinerea	370	259	111
P. brassicae	659	517	142
V. longisporum	3222	1862	1360

A small number of GEMs are associated with both PAMP-induced defence response and QDR

The extent to which QDR is related to PTI is unknown. However, studies suggest correlations between PTI and QDR responses (Vetter *et al.*, 2012; Samira *et al.*, 2020) and some QDR genes are associated with perception and initial signalling responses of PTI (Lacombe *et al.*, 2010). Considering this, we hypothesised that there would be a correlation between phenotypic responses to PAMPs (ROS response) and QDR. In addition, we hypothesised that there would be shared GEMs associated with PTI and QDR to the fungal pathogens.

Flg22 produces a strong and repeatable ROS response in many plant species and is often used to study PTI even alongside unrelated fungal pathogens (Ferrari *et al.*, 2007; Samira *et al.*, 2020). Chitin is a fungal PAMP; thus, it is the most appropriate elicitor for our study, and we previously developed robust methods—including quantification of chitin-induced ROS—to measure PTI in *B. napus* (Lloyd et al., 2014). Nevertheless, first we wanted to confirm that chitin-induced ROS response was quantitative and reproducible in our *B. napus*

population. Furthermore, we hypothesised that there would be an overlap in the phenotypic responses and GEMs associated with PTI responses to PAMPS chitin, flg22, and elf18.

The *B. napus* genotypes demonstrated varying levels of PAMP-induced ROS production with all three PAMPs, suggesting that—like resistance to the fungal pathogens—these were quantitative traits (Fig. **2a, S1a**). We produced a correlation matrix which indicated that the *B. napus* genotypes ranked similarly in their response to different PAMPs (Fig. **2b**). We did not identify any significant GWA marker associations for any PAMP using a false discovery rate of 0.05 (Table **S2**). However, we identified 184, 286, and 3251 GEMs associated with chitin-, flg22-, and elf18-induced ROS response, respectively (Table **S3**). We did not find any known PRRs in our datasets, although this is unsurprising since mutations in PRRs probably cause a qualitative phenotype. There was a significant overlap between GEMs associated with the PAMP responses. For example, out of the 184 chitin-induced ROS GEMs, 31% were shared with the flg22 response, 54% were shared with the elf18 response, and 21% were shared with both flg22 and elf18 responses (Table **S4,** Fig. **S1b**). These data suggest that response to PAMPs has some general genetic control and some PAMP-dependent distinct elements. Since our study is based on fungal pathogens and ROS response to chitin presented a quantitative phenotype with a considerable number of significantly associated GEMs, we focused the following investigations on the overlap between chitin-associated and QDR-associated loci.

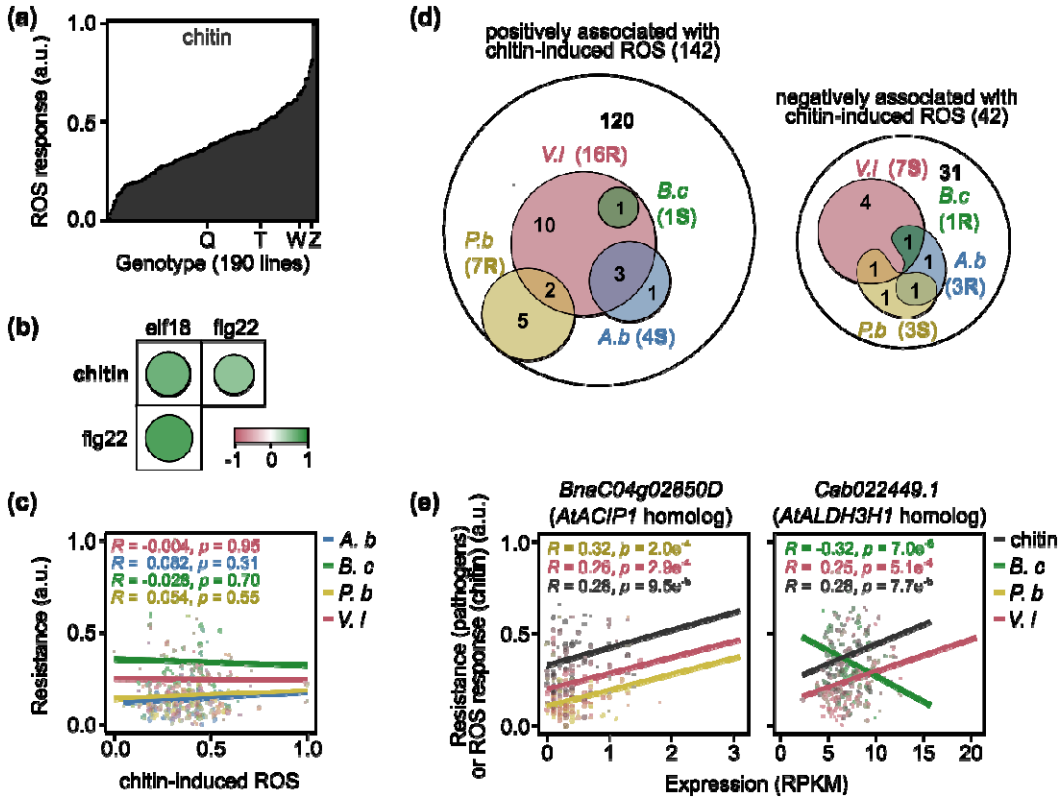

Fig. 2. Relationship between chitin-induced ROS and *B. napus* quantitative disease resistance. (a) Chitin-induced ROS response (arbitrary units (a.u.), normalized values between zero and one) of different *B. napus* genotypes. The positions of reference genotypes Quinta (Q), Tapidor (T), Westar (W) and Zhongshuang 11 (Z) are indicated. (b) Correlation between the PAMP-induced ROS responses of *B. napus* lines elicited by chitin, flg22, and elf18. Positive correlations (green) are indicated between pair-wise comparisons of ROS responses. (c) Linear regression analysis of chitin-induced ROS response relative to quantitative disease resistance to *Alternaria brassicicola (A.b), Botrytis cinerea (B.c)*, *Pyrenopeziza brassicae (P.b)* or *Verticillium longisporum (V.l)* (arbitrary units (a.u.), normalized values between zero and one). (d) The number of gene expression markers (GEMs) whose expression was positively or negatively associated with chitin-induced ROS and the number which were also associated with resistance (R) or susceptibility (S) to the *B. napus* fungal pathogens. Venn diagram indicating the overlap between GEMs associated with several pathogen interactions. (e) Linear regression analysis of gene expression (RPKM) of *BnaC04g2850D* and *Cab022449.1* relative to chitin-induced ROS responses and resistance to fungal pathogens.

We hypothesised that variation in the ROS response elicited by chitin would be correlated to QDR. We plotted chitin-induced ROS response relative to QDR response to *A. brassicicola, B. cinerea, P. brassicae* and *V. longisporum.* However, we observed no overall correlation between ROS response and QDR response in the *B. napus* genotypes. (Fig. **2c**). Nevertheless, we hypothesised that some QDR GEMs may relate to PTI. We compared the GEMs associated with resistance to fungal pathogens with those associated with chitin-induced ROS (Table **S4**). We found that only a small percentage (<1%) of the total number of QDR GEMs for each pathogen related to chitin-induced ROS response. We did an enrichment analysis based on the hypergeometric probability formula (Plaisier *et al.*, 2010) to determine if the number of GEMs shared between chitin-induced ROS response and QDR to each fungal pathogen was greater than the number that would be expected by chance. There was no significant enrichment in the number of GEMs shared between chitin-induced ROS response and QDR to both necrotrophic pathogens and only a slight but significant enrichment in the number of GEMs shared between chitin-induced ROS response and QDR to both hemibiotrophic pathogens (Table **S5**). Overall, these data, indicate that the majority of QDR is not associated with the genes potentially affecting the magnitude of PAMP-induced ROS response (Fig. **S1c**).

Despite the lack of overlap between GEMs associated with QDR and chitin-induced ROS response, we still identified a few GEMs associated with both processes. Of the 184 GEMs that were associated with chitin-induced ROS, 142 were positively associated, i.e., increased gene expression was associated with the increased magnitude of chitin-induced ROS response. Of these, seven GEMs were associated with resistance to *P. brassicae* and 16 GEMs were associated with resistance to *V. longisporum* (Fig. **2d**, Table **2**). These included *BnaC04g02850D*—a homolog of *A. thaliana ACIP1* (Fig. **2e**)—which was also associated with flg22 and elf18 responses (Table **S4**). In contrast, four GEMs were associated with susceptibility to *A. brassicicola* and one GEM was associated with susceptibility to *B. cinerea*. Interestingly, the expression of *Cab022449.1*—a homolog of *A. thaliana Aldehyde dehydrogenase 3H1 (ALDH3H1)*—was positively associated with chitin-induced ROS and resistance

to *V. longisporum* but associated with susceptibility to *B. cinerea* (Fig**. 2e**). Forty-two GEMs were negatively associated with chitin-induced ROS response, i.e., decreased gene expression was associated with an increased magnitude of chitin-induced ROS response. Of these, three GEMs were associated with resistance to *A. brassicicola* and one GEM was associated with resistance to *B. cinerea* (Fig. **2d**, Table **2**). In contrast, seven GEMs were associated with susceptibility to *V. longisporum,* and three GEMs were associated with susceptibility to *P. brassicae*.

Table 2 The numbers of GEMs positively and negatively associated with chitin-induced ROS response and associated with either resistance (R) or susceptibility (S) to *Brassica napus* fungal pathogens *Alternaria brassicicola, Botrytis cinerea, Pyrenopeziza brassicae* or *Verticillium longisporum.* The direction of the correlation (positive or negative) of QDR GEMs compared to the chitin-induced ROS GEMs is also summarized.

	GEMs positively correlated with chitin-induced ROS (142)		GEMs negatively correlated with chitin-induced ROS (42)		
Pathogen	Number	Type (R/S)	Number	Type (R/S)	Correlation to chitin-induced ROS GEMs
A. brassicicola	4	S	3	R	7 -ve
B. cinerea	1	S	1	R	2 -ve
P. brassicae	7	R	3	S	10 +ve
V. longisporum	16	R	7	S	23 +ve

Of the 31 GEMs overlapping between fungal resistance and chitin-induced ROS, 27 were associated with response to elf18 and 12 were associated with response to flg22 suggesting that these GEMS are associated with the magnitude of ROS response rather than PAMP specificity. In summary, here we identified GEMs where increased expression was correlated to increased ROS response, increased QDR to *P. brassicae* and *V. longisporum,* but decreased QDR to *A. brassiciciola* and *B. cinerea.* In addition, we identified GEMs where decreased expression was correlated to decreased ROS response, decreased QDR to *P. brassicae* and *V. longisporum,* but increased QDR to *A. brassiciciola* and *B. cinerea* (Fig. **2d**).

Brassica napus QDR gene expression markers are associated with broad-spectrum resistance

We hypothesised that if broad-spectrum QDR was present in the *B. napus* population, there could be a correlation between some phenotypic responses to the different pathogens and some common associated GEMs which could be interesting targets for breeding. To determine any correlation between the QDR response of *B. napus* genotypes to different fungal pathogens, we produced a matrix of the correlation strength between pair-wise comparisons of fungal pathogens (Fig. **3a**). There was a positive correlation between resistance to *A. brassicicola* and resistance to *B. cinerea.* However, there was a negative correlation between resistance to *V. longisporum* and resistance to necrotrophic pathogens *A. brassicicola* and *B. cinerea* and between resistance to *P. brassicae* and resistance to *B. cinerea.*

To identify GEMs associated with QDR to several pathogens, we did comparisons between the lists of resistance GEMs and between the lists of susceptibility GEMs for the fungal pathogens (Fig. **3b**) and performed enrichment analyses. There was a significant enrichment in the number of GEMs shared between *Alternaria brassicicola* and *B. cinerea* (73 resistance GEMs and 56 susceptibility GEMs) and the number of GEMs shared between *Pyrenopeziza brassicae* and *V. longisporum* (89 resistance GEMs and 42 susceptibility GEMs) (Table **S5**, **S6**). Interestingly, neither of the necrotrophic pathogens (*A. brassicicola* and *B. cinerea*) shared any resistance or susceptibility GEMs with those from the hemibiotrophic pathogens (*P. brassicae* and *V. longisporum*).

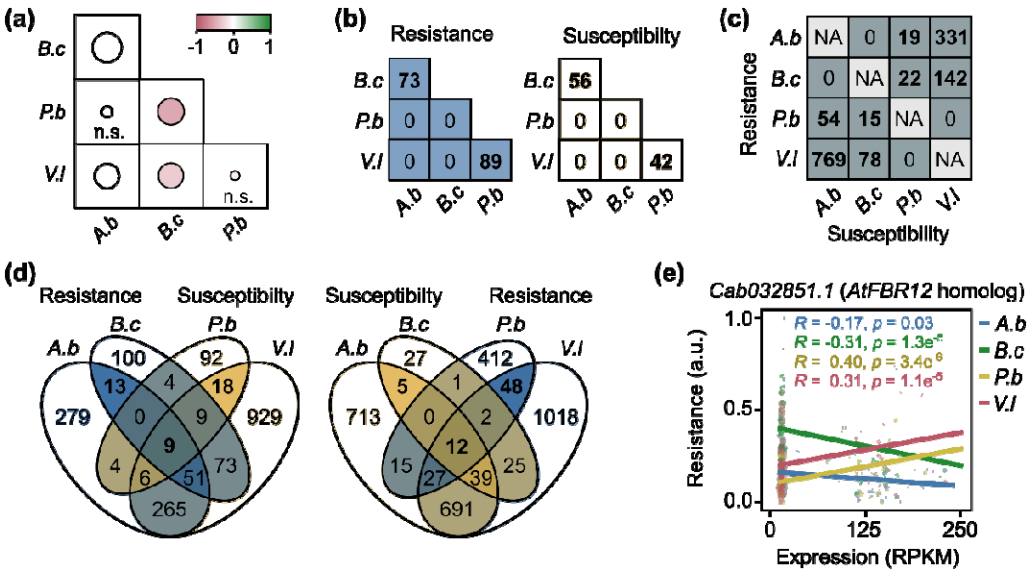

Fig. 3 *Brassica napus* lines have common defence mechanisms against several fungal pathogens. (a) Correlation between the resistance phenotype of *B. napus* lines to fungal pathogens *Alternaria brassicicola (A.b)*, *Botrytis cinerea (B.c)*, *Pyrenopeziza brassicae (P.b)* or *Verticillium longisporum (V.l).* Positive correlations (green), negative correlations (red) and no correlation (n.s.); strengths of correlation (sizes of circles) are indicated between pair-wise comparisons of resistance responses. (b) The numbers of resistance (blue) and susceptibility (yellow) gene expression markers (GEMs) shared between pair-wise comparisons of pathogens. (c) The numbers of GEMs associated with resistance to one pathogen and susceptibility to another pathogen. (d) Venn diagrams showing the overlap between *A.b and B.c* susceptibility GEMs and *P.b* and *V.l* resistance GEMs (right) and the overlap between *A.b and B.c* resistance GEMs and *P.b* and *V.l* susceptibility GEMs (left). (e) Linear regression analysis of gene expression (RPKM) of *Cab032851.1* relative to resistance to fungal pathogens (arbitrary units (a.u.), normalized values between zero and one).

Hemibiotrophic pathogens and necrotrophic pathogens utilize different plant mechanisms to facilitate their infection, and previous studies have identified specific genes involved in resistance to hemibiotrophic pathogens which confer susceptibility to necrotrophic pathogens (Lorang *et al.,* 2007). Thus, we hypothesised that there might be QDR GEMs with antagonistic associations dependent on the lifestyle of the pathogen. We compared resistance GEMs with susceptibility GEMs for each pair-wise combination of fungal pathogens (Fig. **3c**). As expected, we found no GEMs with antagonistic effects for the pair of necrotrophic pathogens and the pair of hemibiotrophic pathogens. Interestingly,

there was a significant enrichment of GEMs associated with antagonistic effects on resistance for necrotrophic and hemibiotrophic pathogens; for example, 1100 (769 + 331) GEMs with opposite effects on resistance were associated with *A. brassicicola* and *V. longisporum* (Table **S5, S6**).

To identify broad-spectrum resistance GEMs with no antagonistic effects on susceptibility to other pathogens, we compared shared susceptibility GEMs for *A. brassicicola* and *B. cinerea* with shared resistance GEMs for *P. brassicae* and *V. longisporum.* We also compared shared resistance GEMs from *A. brassicicola* and *B. cinerea* with shared susceptibility GEMs from *P. brassicae* and *V. longisporum* (Fig. **3d,** Table **S5**). 18 GEMs (13 + 5) were associated with resistance or susceptibility to both *A. brassicicola* and *B. cinerea* with no significant associations to *P. brassicae* and *V. longisporum* (Table **3**). 66 GEMs (48 + 18) were associated with resistance or susceptibility to both *P. brassicae* and *V. longisporum* with no significant associations with *A. brassicicola* and *B. cinerea* (Table **4**).

Interestingly, there was a significant enrichment of GEMs associated with susceptibility or resistance to both *A. brassicicola* and *B. cinerea* with opposing associations for susceptibility or resistance to *P. brassicae* and *V. longisporum:* 21 GEMs (9 + 12) (Table **5, S6**). These GEMs are interesting from a mechanistic viewpoint. For example, the expression of *Cab032821.1*—the homolog of *A. thaliana Fumosin B1-resistant 12, FBR12*—was associated with resistance to both *P. brassicae* and *V. longisporum* but susceptibility to both *A. brassicicola* and *B. cinerea* (Fig. **3e**). The expression of *Bo8g081460.1*—the homolog of an *A. thaliana* disease resistance nucleotide-binding leucine-rich repeat (NBS-LRR) protein—was also associated with resistance to the hemibiotrophic pathogens and susceptibility to the necrotrophic pathogens (Table **5**).

Table 3. Broad-spectrum GEMs associated with resistance (R) or susceptibility (S) to necrotrophic fungi (necro.) *Alternaria brassicicola* and *Botrytis cinerea,* with no antagonistic effects on hemibiotrophic fungi (hemi.) *Pyrenopeziza brassicae* and *Verticillium longisporum.* The putative *Arabidopsis thaliana* (*At*) orthologs, protein class, and gene ID are indicated.

GEM	Necro.	Hemi.	*At* ortholog	Gene name	Protein class
Cab019641.1	R	-	-	-	-
Cab029666.1	R	-	AT1G04980.1	*PDI10; Protein disulfide-isomerase like 2-2*	chaperone
Cab006731.1	R	-	-	-	-
Cab023848.3	R	-	AT3G13772.1	*TMN7; Transmembrane 9 superfamily member 7*	transporter
Bo6rg071140.1	R	-	AT3G56460.1	*GroES-like zinc-binding alcohol dehydrogenase family protein*	oxidoreductase
Cab006719.1	R	-	AT5G24630.5	*BIN4; Brassinosteroid insensitive 4*	DNA-binding
Bo3g028280.1	R	-	AT4G38220.2	*AQI, Aquaporin interactor, N-acyl-L-amino-acid amidohydrolase*	-
Bo9g183340.1	R	-	AT5G02820.1	*BIN5, Brassinosteroid insensitive 5, DNA topoisomerase 6 subunit A*	endodeoxyribonuclease
Bo3g004890.1	R	-	AT5G08380.1	*AGAL1; Alpha-galactosidase 1*	galactosidase
Cab010087.2	R	-	-	-	-
Cab023861.2	R	-	AT1G72730.1	*Eukaryotic initiation factor 4A-3*	RNA helicase
BnaC03g41840D	R	-	-	-	-
Bo1g017790.1	R	-	AT4G17720.1	*BPL1; Putative RRM-containing protein*	RNA splicing factor
Cab007046.1	S	-	AT5G48590.1		
Bo5g132170.1	S	-	AT3G13740.1	*RNC4; RNase III-like enzyme*	
Cab029917.1	S	-	AT1G01090.1	*PDH-E1 ALPHA; Pyruvate dehydrogenase E1 subunit alpha-3*	dehydrogenase
Bo3g040470.1	S	-	AT2G27510.1	*FD3; Ferredoxin-3*	reductase
Bo5g132390.1	S	-	AT3G13550.1	*COP10, Constitutive photomorphogenesis protein 10*	ubiquitin-protein ligase

Table 4. Broad-spectrum GEMs associated with resistance (R) or susceptibility (S) to hemibiotrophic fungi (hemi.) *Pyrenopeziza brassicae* and *Verticillium longisporum,* with no antagonistic effects on necrotrophic fungi (necro.) *Alternaria brassicicola* and *Botrytis cinerea.* The putative *Arabidopsis thaliana* (*At*) orthologs, protein class, and gene ID are indicated. Multiple GEMs corresponding to *A. thaliana* ortholog AT3G09980.1 are highlighted.

GEM	Necro.	Hemi.	*At* ortholog	Gene name	Protein class
BnaC09g43580D	-	R	-	-	-
Cab025354.2	-	R	AT2G45580.1	*CYP76C3; Cytochrome P450, family 76, subfamily C, polypeptide 3*	-
Bo4g182630.1	-	R	AT2G34470.1	*UREG; Urease accessory protein G*	-
Bo5g058580.1	**-**	**R**	**AT3G09980.1**	***ACIP1; Acetylated interacting protein 1***	**-**
Bo4g183100.1	-	R	AT2G35190.1	*NPSN11; Novel plant SNARE 11*	SNARE protein
Bo2g095510.1	-	R	AT1G80930.1	*Pre-mRNA splicing factor CWC22 homolog*	RNA processing factor
Bo9g176470.1	-	R	AT5G06250.2	*NGAL3; NGATHA-like protein 3, B3 domain-containing protein*	transcription factor
BnaC03g64760D	**-**	**R**	**AT3G09980.1**	***ACIP1; Acetylated interacting protein 1***	**-**
Cab042580.1	-	R	AT4G02710.1	*NET1C; Protein NETWORKED 1C, Ki-se interacting (KIP1-like)*	-
Bo4g045470.1	-	R	AT2G32860.1	*BGLU33; beta glucosidase 33*	-
Bo4g182440.1	-	R	AT2G34250.2	*SecY/Sec61-alpha family member protein*	transporter
Cab042707.1	-	R	AT5G51120.1	*PAMN1; Polyadenylate-binding protein 1 homolog*	translation initiation factor
Cab037277.2	-	R	AT3G22550.1	*FLZ8; FCS-Like Zinc finger 8*	-
Bo4g183310.1	-	R	AT2G35510.1	*SRO1, Similar to RCD 1, I-ctive poly [ADP-ribose] polymerase*	-
Cab025625.4	-	R	-	-	-
Bo6rg103690.1	-	R	AT1G67280.2	*GLYI6; Lactoylglutathione lyase*	lyase
Bo4g182680.1	-	R	-	-	-
Bo2g095560.1	-	R	-	-	-
Cab029121.1	-	R	AT2G26250.1	*KCS10; 3-ketoacyl-CoA synthase 10*	-
Bo5g137820.1	**-**	**R**	**AT3G09980.1**	***ACIP1; Acetylated interacting protein 1***	-
Bo4g194830.1	-	R	AT2G44120.1	*60S ribosomal protein L7-3*	ribosomal protein
Cab013800.1	-	R	AT1G16445.1	*S-adenosyl-L-methionine-dependent methyltransferases superfamily*	methyltransferase
Bo2g095550.1	-	R	-	-	-
Bo4g182550.1	-	R	AT2G34410.2	*RWA3; Reduced wall acetylation 3 homolog*	-
Bo4g182960.1	-	R	AT2G34840.1	*epsilon2-COP; Coatomer subunit epsilon-2*	vesicle coat protein
Bo1g051850.1	-	R	AT2G31290.2	*Ubiquitin carboxyl-terminal hydrolase family protein*	-
BnaC06g39270D	-	R	-	-	-
Bo1g003050.1	-	R	AT4G40000.1	*TRM4A; S-adenosyl-L-methionine-dependent methyltransferase*	R- methyltransferase
Bo4g023900.1	-	R	AT2G44620.1	*Acyl carrier protein 1, mitochondrial*	-
Cab002494.2	-	R	AT2G30320.1	-	-
Cab007584.1	-	R	AT5G05800.2	*L10-interacting MYB domain-containing protein*	-

GEM	Necro.	Hemi.	*At* ortholog	Gene name	Protein class
BnaC04g02850D	**-**	**R**	**AT3G09980.1**	***ACIP1; Acetylated interacting protein 1***	**-**
BnaC05g07480D	-	R	-	-	-
Bo5g003800.1	-	R	AT1G03365.1	*Putative E3 ubiquitin-protein ligase RF4*	-
Cab042031.1	-	R	-	-	-
Bo4g183270.1	-	R	-	-	-
Bo4g183070.1	-	R	AT2G35050.1	*Kinase superfamily domain-containing protein*	non-receptor ser/thr kinase
Bo4g182310.1	-	R	AT2G33860.1	*ARF3/ETT; Auxin response factor 3/ETTIN*	-
Cab019919.4	-	R	AT4G31040.1	*DLDG1; Chloroplast envelope membrane protein*	-
Bo6rg003510.1	-	R	AT3G18524.1	*MSH2; DNA mismatch repair protein*	D- metabolism protein
Cab019786.1	-	R	AT4G29530.1	*THMPASE1; Thiamine phosphate phosphatase-like protein*	phosphatase
Bo4g182420.1	-	R	AT3G18430.2	*Calcium-binding EF-hand family protein*	-
Bo6rg003540.1	-	R	AT1G44790.1	*Gamma-glutamylcyclotransferase 2-3*	-
Cab007776.1	-	R	AT5G11710.1	*EPS1; Clathrin interactor EPSIN 1*	membrane trafficking
Bo4g183130.1	-	R	AT2G35230.1	*IKU1; Protein HAIKU1*	-
Bo4g143960.1	-	R	AT5G37890.1	*SI-L7; E3 ubiquitin-protein ligase SI--like 7*	ubiquitin-protein ligase
Cab007778.1	-	R	-	-	-
Bo6rg003520.1	-	R	AT1G44770.1	*elongation factor*	-
Cab019945.1	-	S	-	-	-
Cab044891.1	-	S	-	-	-
BnaA08g28590D	-	S	-	-	-
Bo6rg033210.1	-	S	AT1G55090.1	*Glutamine-dependent -D(+) synthetase*	ligase
BnaC08g18360D	-	S	-	-	-
Bo2g007540.1	-	S	AT5G07210.1	*ARR21; Putative two-component response regulator 21*	transcription factor
BnaA01g02330D	-	S	-	-	-
Cab002672.1	-	S	AT2G33810.1	*SPL3; Squamosa promotor binding protein-like 3*	DNA-binding
Cab013528.1	-	S	-	-	-
Cab034921.1	-	S	AT2G38540.1	*LP1; Non-specific lipid-transfer protein 1*	-
Cab020282.2	-	S	-	-	-
Bo7g095690.1	-	S	AT5G25830.1	*GATA12; GATA transcription factor 12*	transcription factor
BnaC08g15170D	-	S	-	-	-
Cab037036.1	-	S	-	-	-
Cab034089.1	-	S	-	-	-
Bo8g087140.1	-	S	AT3G54890.1	*LHCA1; Light-harvesting complex gene 1*	-
Bo6rg098720.1	-	S	AT1G67700.1	*HHL1; Hypersensitive to high light 1*	-
Bo5g152840.1	-	S	AT3G02150.2	*PTF1; Plastid transcription factor 1*	transcription factor

Table 5. Broad-spectrum GEMs associated with resistance (R) or susceptibility (S) to hemibiotrophic fungi (hemi.) *Pyrenopeziza brassicae* and *Verticillium longisporum,* with antagonistic effects on necrotrophic fungi (necro.) *Alternaria brassicicola* and *Botrytis cinerea.* The putative *Arabidopsis thaliana* (*At*) orthologs, protein class, and gene ID are indicated.

GEM	Necro.	Hemi.	*At* ortholog	Gene name	Protein class
BnaA10g08980D	R	S	AT2G34470.2	*UREG; Urease accessory protein G*	
Bo2g101920.1	R	S	AT3G10020.1	*HUP26; Hypoxia unknown protein 26*	
Cab002732.1	R	S	-	-	
Bo2g101910.1	R	S	-	-	
Bo4g021310.1	R	S	AT2G44150.1	*ASHH3; Histone-lysine N-methyltransferase*	
BnaA06g22180D	R	S	-	-	
Bo7g077710.1	R	S	AT5G47570.1	*NADH dehydrogenase ubiquinone 1 beta subcomplex subunit*	dehydrogenase
Cab031167.1	R	S	-	-	
Cab017493.1	R	S	AT5G56940.1	*Ribosomal protein S16 family protein*	ribosomal protein
Cab007887.1	S	R	AT5G13310.1	-	
Bo6rg081580.1	S	R	AT1G78420.2	*DA2; mono-ubiquitinator*	
Bo9g176310.1	S	R	AT5G06310.1	*POT1b, Protection of telomeres 1b*	DNA metabolism protein
Cab029870.1	S	R	AT1G02560.1	*CLPP5; Nuclear encoded Clp protease 5*	serine protease
Bo6rg081770.1	S	R	AT1G78170.1	*EAU1, Ethylene-responsive element binding factor-associated*	
Cab032816.1	S	R	AT1G24170.1	*LGT9, Galacturonosyltransferase-like 8*	glycosyltransferase
Cab027999.1	S	R	-	-	
Cab018896.1	S	R	AT1G76610.1	*MIZU-KUSSEI-like protein*	
Bo4g151450.1	S	R	-	-	
Bo8g081460.1	S	R	AT3G51570.1	*Disease resistance protein (TIR-NBS-LRR class)*	
Cab032851.1	S	R	AT1G26630.1	*FBR12; Fumonisin B1-resistant 12*	translation initiation factor
Bo4g149580.1	S	R	AT2G22400.1	*TRM4B, S-adenosyl-L-methionine-dependent methyltransferases*	RNA methyltransferase

***Brassica napus* resistance *to Verticillium longisporum* is associated with a genomic deletion on chromosome A09.**

Although the GWA analysis in our study did not produce any significant results, we hypothesised that combining the information from GWA and GEM analyses—such as comparing minor peaks from GWA analyses with highly significant GEMs—might be a powerful tool to identify strong candidate QDR genes.

We compared the most significant GEMs associated with resistance to each pathogen with the greatest associations from GWA. We observed that the greatest GWA association for resistance to *V. longisporum* (SNP marker Cab013526.1.135.A) also corresponded to a highly significant GEM (*Cab013526.1*) (Fig. **4a**). Assessment of phenotypic variation segregating with alleles for Cab013526.1.135.A revealed that accessions inheriting a “G” at this locus had resistance values ~43% less than those accessions inheriting an “A” (Fig. **4b**). We calculated the distance in LD with this marker and found a region of 0.51 MB containing 107 genes (Fig. **4c**). We plotted the significance of *V. longisporum* resistance GEMs as a function of their distance along the chromosome and found that *Cab013526.1* belonged to a peak of five genes (*Cab013522.1, Cab013524.1, Cab013523.1, Cab013526.1,* and *Cab013517.1*), suggesting that the expression of all five genes in the region is associated with resistance to *V. longisporum*. (Fig. **4d**).

Since the expression of five GEMs in proximity was associated with resistance to *V. longisporum*, we hypothesised that this association may be the result of a genomic deletion in this region. To investigate this, we first examined the data across the association panel to determine if there were genotypes with low gene expression and high susceptibility. Within our dataset, published genomes were available for: Quinta, Tapidor, Westar and Zhongshuang 11 (Song *et al.*, 2020). Quinta had little resistance to *V. longisporum* and very low expression of the five GEMs (expression at such levels could be a result of cross-mapping to the homoeologous region on the *B. napus* ‘C’ genome, C08) (Fig. **4e**). On the other hand, Tapidor, Westar, and Zhongshuang 11 exhibited moderate resistance and gene expression levels. We hypothesised that Quinta has a

deletion on *B. napus* chromosome A09, whereas Tapidor, Westar, and Zhongshuang 11 have not.

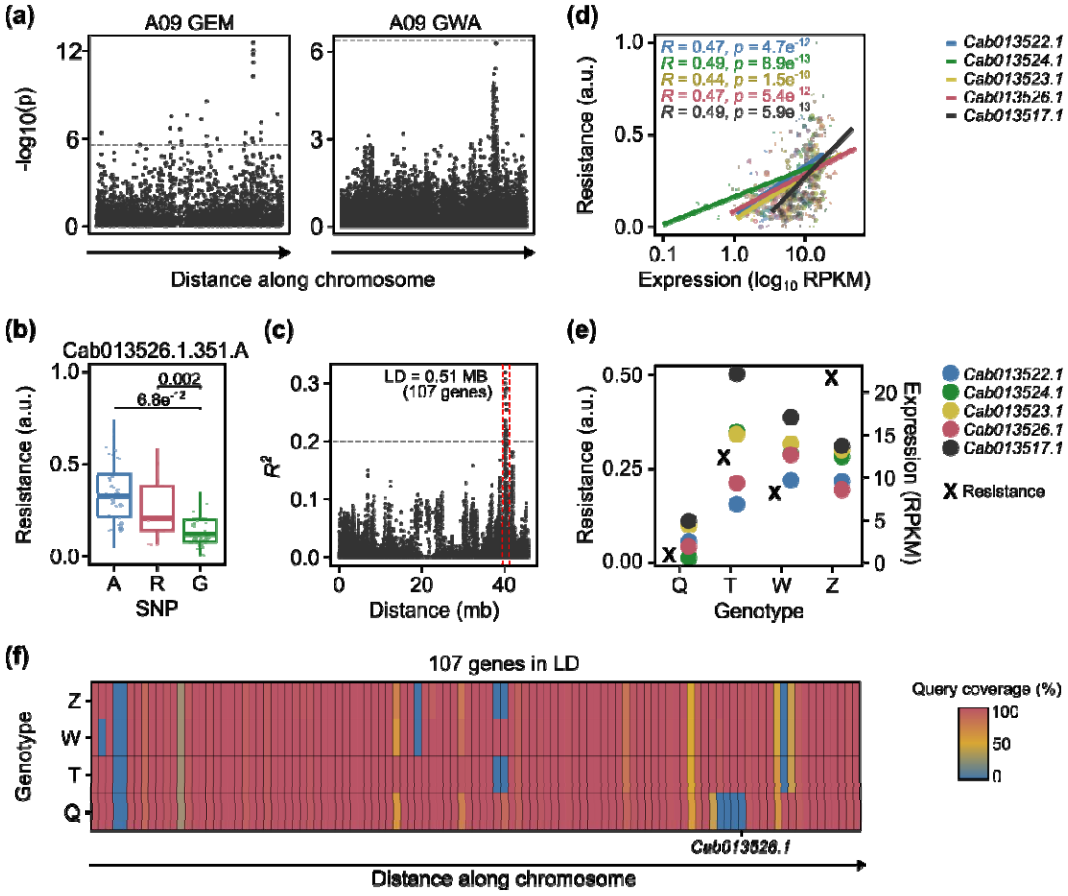

Fig. 4 Resistance *to Verticillium longisporum* is associated with a genomic deletion on chromosome A09. (a) Manhattan plots showing marker-trait association resulting from GEM and GWA analysis of resistance to *V. longisporum* in 191 *Brassica napus* genotypes. The x-axis indicates GEM or SNP location along the chromosome; the y-axis indicates the -$\log_{10}$(p) (*P* value). (b) Segregation of resistance to *V. longisporum* (arbitrary units (a.u.), normalized values between zero and one) with the highest associating marker, Cab013526.1.651.A, show a marker effect of 20% between A and G (R = A/G). *P* values were determined by a Student's t-test. (c) Linkage decay plot from marker Cab013526.1.651.A as a function of genetic distance (MB). The grey line indicates an R^2 value of 0.2, red lines indicate the area of linkage disequilibrium. (d) Linear regression analysis of gene expression ($\log_{10}$ RPKM) of the five highest associating Gene expression markers (GEMs) relative to resistance to *V. longisporum* in 191 *B. napus* genotypes GEMs *Cab013522.1, Cab013524.1, Cab013523.1, Cab013526.1* and *Cab013517.1* are displayed in order of significance from GEM analyses. (e) Resistance to *V. longisporum* (left-hand y-axis) and gene expression (RPKM) of the five highest associating GEMs (right-hand y-axis) in reference genotypes Quinta (Q), Tapidor (T), Westar (W) and

Zhongshuang 11 (Z). (f) Heatmap indicating query coverage (compared to the *B. napus* pantranscriptome) in Q, T, W and Z for the 107 genes predicted to be in linkage disequilibrium with Cab013526.1.651.A on chromosome A09.

For each reference genotype, we did a BLAST analysis against the *B. napus* pantranscriptome for the 0.51 MB (107 genes) region in LD with the most significant SNP marker to determine the query coverage of these 107 genes (Fig. **4f**). We hypothesised that there would be conserved regions in Tapidor, Westar, and Zhongshuang 11 that were not conserved in Quinta. Five consecutive genes showed ~100 % query coverage for Tapidor, Westar, and Zhongshuang 11 but reduced query coverage in Quinta: *Cab013522.1* (40%), *Cab013523.1* (0%), *Cab013524.1* (0%), *Cab013525.1* (0%), *Cab013526.1* (0%) (Table **S7**). We did the BLAST analysis against the homoeologous region on chromosome C08 and observed no differences in Quinta compared to the other three reference genotypes, suggesting that this deletion was specific to chromosome A09 (Fig. **S2a**). These data suggest that one or more of these five genes is associated with QDR to *V. longisporum.* Alternatively, downstream of these five genes was a region including two genes with ~100 % query coverage in Quinta but reduced query coverage in Tapidor, Westar, and Zhongshuang 11: *BnaA09g43290D* (0 %) and *Cab013532.1* (40%). However, neither was a GEM associated with resistance to *V. longisporum*; thus, we speculated that it was unlikely that either was a candidate susceptibility gene (Table **S2**).

To understand which gene/genes in the potential deletion may have a role in resistance to *V. longisporum,* we hypothesized that—for the causal gene/genes—their homologs in the *B. napus* genome may also be GEMs for resistance to *V. longisporum.* Each of the five genes on A09 only had one homolog, on chromosome C08. None of their five homologs were significant GEMs; however, linear regression analysis of gene expression relative to *V. longisporum* resistance indicated a significant association for the Cab013522.1 homolog (Bo8g101810.1) and Cab013524.1 homolog (Bo8g101830.1) (Fig. **S2b**). Interestingly, Cab013522.1, Cab013524.1, and Cab013526.1 were also GEMs associated with resistance to *P. brassicae* and Cab013522.1, Cab013523.1, Cab013524.1, and Cab013526.1 were associated with susceptibility to *A. brassicicola*, indicating that one or more could be candidates

for broad-spectrum resistance with potential trade-offs for susceptibility to *A. brassicicola*.

To understand the potential function of the five genes in the deletion, we identified their putative *A. thaliana* orthologs using BLAST (**Table 6**). The orthologs included a microtubule-binding motor protein, *Kinesin motor family protein, KIN7.2* (Cab013522.1); a carbohydrate kinase, *Xylulose kinase 1, XK1* (Cab013523.1); a multidrug and toxin extrusion (MATE) transporter, *Enhanced disease susceptibility 5 homolog, EDS5H* (Cab013524.1)*;* a plastid isoform aldolase, *Fructose-bisphosphate aldolase 1, FBA1* (Cab013525.1)*;* and a B-box zinc finger family transcription factor, *B-box domain protein 18, BBX18* (Cab013526.1).

Table 6. The five genes in the deletion on chromosome A09 associated with resistance against *Verticillium longisporum*. The putative *Arabidopsis thaliana* (*At*) orthologs, protein class, and gene ID are indicated.

GEM	*At* ortholog	Gene name	Protein class
Cab013522.1	AT2G21380.1	***KIN7.2****; Kinesin motor family protein*	microtubule binding motor protein
Cab013523.1	AT2G21370.2	***XK1****, Xylulose kinase 1*	carbohydrate kinase
Cab013524.1	AT2G21340.2	***EDSH5****, Enhanced disease susceptibility 5 homolog*	transporter (MATE efflux protein)
Cab013525.1	AT2G21330.1	***FBA1****; Fructose-biphosphate aldolase 1*	aldolase
Cab013526.1	AT2G21320.1	***BBX18****; B-box domain protein 18*	zinc family transcription factor

Discussion

In this study, we used an AT pipeline to investigate QDR to *B. napus* fungal pathogens: *A. brassicicola, B. cinerea, P. brassicae* and *V. longisporum.* We showed evidence of QDR in the *B. napus* population to the four fungal pathogens since we observed a continuous distribution of resistance phenotypes. We investigated a strong candidate region associated with QDR to *V. longisporum*; considered whether QDR loci relate to PTI; and determined loci associated with broad-spectrum resistance.

Broad-spectrum QDR is an opportunity for crop breeding

Our AT analysis enabled us to investigate common and unique gene loci associated with resistance or susceptibility to several pathogens for the first time. We observed a positive correlation between the resistance phenotypes of the *B. napus* genotypes to necrotrophic pathogens *A. brassicicola* and *B. cinerea* and numerous GEMs associated with resistance or susceptibility to both pathogens, suggesting a large overlap of the components affecting defence responses. This is unsurprising since there is a significant overlap between factors that promote colonization by both pathogens—both kill host cells and proliferate on nutrients from dead or dying tissues albeit by different mechanisms. In contrast, we did not observe a correlation between the resistance phenotypes of the *B. napus* genotypes to the hemibiotrophic pathogens *P. brassicae* and *V. longisporum.* This may reflect the differences between phenotyping methods since *P. brassicae* infects leaves and disease severity is scored as sporulation at a single time point, whereas *V. longisporum* infection is an infection of the xylem system and scored as disease progression on stems over time. This does not negate the presence of shared QDR mechanisms; in fact, we identified 131 GEMs associated with resistance against or susceptibility to both pathogens.

Interestingly, there was a negative correlation between the resistance phenotypes of the *B. napus* genotypes to necrotrophic pathogens and hemibiotrophic pathogens, probably due to their differences in infection and feeding strategies. We identified 21 GEMs associated with broad-spectrum

resistance or susceptibility to necrotrophic pathogens with an opposite effect on hemibiotrophic pathogens. Immune responses against biotrophic and hemibiotrophic pathogens—such as cell death response—can be effective at preventing the endophytic growth of *P. brassicae* and *V. longisporum* but could be manipulated by necrotrophic pathogens like *A. brassicicola* and *B. cinerea* to promote infection (McCombe *et al.*, 2022). For example, previous studies indicate that an NBS-LRR gene conferring resistance to biotroph *Puccinia coronata* f. sp. *avenae* is analogous to *LOV1,* a susceptibility factor for necrotrophic pathogen *Cochliobolus victoriae* via programmed cell death (Lorang *et al.,* 2007). In our study, the ortholog of a novel *A. thaliana* NBS-LRR—*Bo8g081460.1*—was associated with resistance to *P. brassicae* and *V. longisporum* and susceptibility to *A. brassicicola* and *B. cinerea.* In addition, the predicted *A. thaliana* ortholog of *FBR12* was associated with resistance to hemibiotrophic pathogens and susceptibility to necrotrophic pathogens and was previously shown to be involved in cell death induced by *Pseudomonas syringae* (Hopkins *et al.*, 2008). Such genes with pathogen-dependent antagonistic associations on susceptibility and resistance to pathogens may not be suitable targets for crop breeding but are interesting mechanistically.

Broad-spectrum disease resistance without trade-offs related to pathogen lifestyle is desirable for crop breeding. We identified GEMs associated with resistance to both *A. brassicicola* and *B. cinerea* with no antagonistic associations with susceptibility to the hemibiotrophic pathogens, including *Brassinosteroid insensitive 4 (BIN4)* and *BIN5.* Interestingly, brassinosteroid signalling has been implicated in resistance or susceptibility to pathogens (De Bruyne *et al.,* 2014); however, *BIN4* and *BIN5* have not been investigated in the context of defence and could be interesting candidates for further study. GEMs associated with resistance to both *P. brassicae* and *V. longisporum* with no antagonistic associations with susceptibility to the necrotrophic pathogens included four GEMs homologous to *A. thaliana ACIP1*— ACIP1 was previously implicated in flg22-induced ROS response and resistance to *Pseudomonas syringae* (Cheong *et al.*, 2014). One of these four was also positively associated with chitin-induced ROS response, highlighting it as a candidate for further investigation into its role in PTI and broad-spectrum QDR. In addition, GEMs

associated with susceptibility to both necrotrophic pathogens with no opposing associations with resistance to the hemibiotrophic pathogens and GEMs associated with susceptibility to both hemibiotrophic pathogens with no opposing associations with resistance to the necrotrophic pathogens could be interesting targets for gene editing since knocking out these genes could increase resistance to the pathogens without the introduction of transgenes (Hua *et al.*, 2019).

A small number of QDR loci relate to PTI

Previous studies have observed correlations between PAMP perception and QDR to pathogens in Arabidopsis (Vetter *et al.*, 2012). In this study, however, we did not observe any correlation between chitin-induced ROS response and resistance to any of the fungal pathogens like that previously reported in sorghum (Samira *et al.*, 2020). Moreover, we found that most GEMs associated with QDR did not relate to ROS production. ROS production is one of the first outputs of PTI; thus, only components upstream of the initial ROS burst would be highlighted in our AT analyses; for example, factors affecting PAMP perception by PRRs and RBOHD-dependent H_2O_2 production. It is possible that other PTI signalling—downstream from initial PAMP perception but divergent from ROS production—may relate to QDR; for example, genes affecting MAPK production and defence gene expression.

Despite the small overlap between chitin-induced ROS and QDR GEMs to the fungal pathogens, we identified several GEMs associated with both. However, additional functional analyses are required to validate the potential role of these genes in both processes. Such GEMs may be PTI components that directly contribute towards QDR by modulating ROS production, or they might have independent functions in PTI and QDR. Furthermore, recent studies indicate that the immune pathways activated by cell-surface PTI and ETI mutually potentiate; for example, activation of PTI PRRs potentiates ETI-induced cell death (Yuan *et al.*, 2021; Ngou *et al.*, 2021), raising the question of whether QDR is also integrated; for example, can PTI enhance QDR?

The *B. napus* ortholog of *A. thaliana ALDH3H1* which was positively correlated to chitin-induced ROS response and *V. longisporum* resistance but negatively correlated to resistance to *B. cinerea*. ALDH proteins—for example, a homolog of *A. thaliana* ALDH3H1, ALDH3I1—can confer tolerance to oxidative stress by scavenging ROS (Kotchoni *et al.*, 2006). PTI-induced rapid ROS production and the accumulation of ROS can lead to programmed cell death which can confer susceptibility to necrotrophic pathogens like *B. cinerea* (Levine *et al.*, 1994; Kotchoni and Gachomo, 2006). *Botrytis cinerea* produces ROS to promote its infection (Govrin and Levine, 2000) and ROS scavengers reduce infection severity (Tiedemann, 1997). Thus, it follows that genotypes with a potentially greater ability to scavenge ROS would be less susceptible to *B. cinerea*. In summary, our data suggests that some GEMs associated with increased ROS response were also associated with increased QDR against hemibiotrophic pathogens but could have trade-offs for resistance against necrotrophic pathogens.

Identification of a novel locus for *V. longisporum* resistance

Combining SNP and gene expression data through AT is a powerful tool for the identification of candidate genes (Havlickova *et al.*, 2018). Here, we identify a novel locus associated with resistance to *V. longisporum* and further in silico analyses of the region indicated five genes within the potential causal genetic deletion. Any of the five genes could be responsible for the resistance phenotype; however, KIN7.2, EDS5H, and BBX18 homologs were also GEMs for resistance to *P. brassicae*, suggesting these could be associated with broad-spectrum QDR. KIN7.2 is involved in microtubule-based movement and—in the animal field—kinesins have been implicated in the trafficking of proteins involved in anti-fungal defence (Kurowska *et al.*, 2012; Ogbomo *et al.*, 2018). EDS5H is a homolog of EDS5, a MATE protein with established functions in plant salicylic acid (SA) dependent defence (Nawrath *et al.*, 2002). However, unlike EDS5, in *A. thaliana* EDS5H is constitutively expressed in green tissues independent of pathogen infection and does not contribute to pathogen-induced SA accumulation (Parinthawong *et al.*, 2015). Nevertheless, MATE proteins can transport a broad range of substrates that could affect QDR, such as organic

acids, plant hormones and secondary metabolites (Nawrath *et al.*, 2002; Takanashi, Shitan and Yazaki, 2014; Su, Rong and Zhang, 2022). On the other hand, BBX18—and the additional two genes in the potential deletion, XK1 and FBA1—have no published associations with defence. Additional functional analyses are needed to validate the deletion and identify the causal gene. Nevertheless, with the in-silico analyses done, we demonstrate the power of the AT pipeline to quickly narrow down on a predicted region of interest for broad-spectrum QDR.

Conclusions

Here, we used an AT pipeline to identify novel loci involved in QDR to several *B. napus* fungal pathogens, *A. brassicicola, B. cinerea, P. brassicicola* and *V. longisporum* and to investigate loci related to both PTI and QDR. We identified several novel GEMs with involvement in PTI and resistance, including those with predicted antagonistic associations with resistance to hemibiotrophic pathogens and necrotrophic pathogens. Furthermore, we highlight several loci with potential roles in broad-spectrum QDR with no antagonistic effects on susceptibility to other pathogens, including a candidate with involvement in PTI, *ACIP1*. In addition, by combining GWA and GEM analyses we were able to identify a novel region of interest for *V. longisporum* resistance. To our knowledge, this is the first time this approach with several pathosystems has been used to identify loci involved in broad-spectrum QDR. In summary, this study provides new insight into broad-spectrum QDR and highlights interesting targets for crop breeding.

Acknowledgements

The authors thank Paweł Jedyński and Tomasz Jęcz (University of Lodz, Poland) for help with plant cultivation and inoculation with *A. brassicicola* and Aiming Qi for advice about *P. brassicae* data analysis. VKM and AKK were supported by the National Center for Research and Development, Poland (grant no. ERA-CAPS II/1/2015). XZ and AvT were supported by the German Research Foundation (grant no. ERA-CAPS DFG; TI170/13–1). HJS, RW, RB, CJR, HF, GKM, HUS and BDLF were funded by the Biotechnology and Biological Sciences Research Council (BBSRC) grants BB/N005007/1 and BB/N005112/1 (as part of the ERA-CAPS consortium "MAQBAT"). HJS, RW, CNJ, RB and CJR were also funded by the John Innes Institute strategic program grants Plant Health BB/P012574/1 (Response BBS/E/J/000PR9796) and Molecules from Nature BB/PO12523/1, Brassica Rapeseed and Vegetable Optimisation (BRAVO) BB/P003095/1.

Competing interests

The authors declare no competing interests

Author contributions

VKM did experiments with *A. brassicicola* infection and analysed the data with AKK. XZ did experiments and data curation with *V. longisporum* infection supervised by AvT. HF and GKM did experiments with *P. brassicae* and analysed data with HUS and HF, HUS and BDLF contributed to the conception and experimental design. RB and HJS did experiments and data curation with *B. cinerea* and PAMPs, HJS contributed to the conception and experimental design, and HJS and CNJ analysed the data. CNJ did statistical analysis of all datasets, CNJ and RW did association transcriptomics, and BS did the BLAST validation of the genomic deletion. CNJ, RW and CJR contributed to the conception, data interpretation and in-silico analyses post-AT. The first draft of the manuscript was written by CNJ, and all authors commented on subsequent versions of the manuscript. All authors read and approved the final manuscript.

Data availability

The R-based GAGA pipeline is available at https://github.com/bsnichols/GAGA. Our population structure is available in Fell *et al.* (2022).

References

Benson JM, Poland JA, Benson BM, Stromberg EL, Nelson RJ. 2015. Resistance to gray leaf spot of maize: genetic architecture and mechanisms elucidated through nested association mapping and near-isogenic line analysis. *PLoS Genetics* **11:** e1005045.

Boschi F, Schvartzman C, Murchio S, Ferreira V, Siri MI, Galván GA, Smoker M, Stransfeld L, Zipfel C, Vilaró FL et al. 2017. Enhanced bacterial wilt resistance in potato through expression of *Arabidopsis* EFR and introgression of quantitative resistance from *Solanum commersonii*. *Frontiers in Plant Science* **8**: 1642.

Bradbury PJ, Zhang Z, Kroon DE, Casstevens TM, Ramdoss Y, Buckler ES. 2007. TASSEL: Software for association mapping of complex traits in diverse samples. *Bioinformatics* **23:** 2633-2635.

Cheong MS, Kirik A, Kim JG, Frame K, Kirik V, Mudgett, MB. 2014. AvrBsT acetylates Arabidopsis ACIP1, a protein that associates with microtubules and is required for immunity. *PLoS Pathogens,* **10:** e1003952.

Corwin JA, Copeland D, Feusier J, Subedy A, Eshbaugh R, Palmer C, Maloof J, Kliebenstein DJ. 2016. The quantitative basis of the *Arabidopsis* innate immune system to endemic pathogens depends on pathogen genetics. *PLoS Genetics* **12:** e1005789.

Corwin JA, Kliebenstein DJ. 2017. Quantitative resistance: more than just perception of a pathogen. *The Plant Cell* **29:** 655-665.

Dakouri A, Lamara M, Karim M, Wang J, Chen Q, Gossen BD, Strelkov SE, Hwang S-F, Peng G, Yu F. 2021. Identification of resistance loci against new

pathotypes of *Plasmodiophora brassicae* in *Brassica napus* based on genome-wide association mapping. *Scientific Reports* **11:** 6599.

De Bruyne L, Höfte M, De Vleesschauwer D. 2014. Connecting growth and defense: the emerging roles of brassinosteroids and gibberellins in plant innate immunity. *Molecular Plant* **7:** 943-959.

Delplace F, Huard-Chauveau C, Dubiella U, Khafif M, Alvarez E, Langin G, Roux F, Peyraud R, Roby D. 2020. Robustness of plant quantitative disease resistance is provided by a decentralized immune network. *Proceedings of the National Academy of Sciences* **117:** 18099-18109.

Deppe, JP, Rabbat R, Hörtensteiner S, Keller B, Martinoia E, Lopéz-Marqués RL. 2018. The wheat ABC transporter Lr34 modifies the lipid environment at the plasma membrane. *Journal of Biological Chemistry* **293:** 18667-18679.

Faris JD, Friesen TL. 2020. Plant genes hijacked by necrotrophic fungal pathogens. *Current Opinion in Plant Biology* **56**: 74-80.

Fell H, Ali AM, Wells R, Mitrousia GK, Woolfenden H, Schoonbeek H-J, Fitt BDL, Ridout CJ, Stotz H. 2022. Novel gene loci associated with susceptibility or cryptic quantitative resistance to *Pyrenopeziza brassicae* in *Brassica napus*. *Theoretical and Applied Genetics,* in press.

Ferrari S, Galletti R, Denoux C, De Lorenzo G, Ausubel FM, Dewdney J. 2007. Resistance to *Botrytis cinerea* induced in Arabidopsis by elicitors is independent of salicylic acid, ethylene, or jasmonate signaling but requires *PHYTOALEXIN DEFICIENT3 Plant Physiology* **144:** 367-379.

Fisher MC, Hawkins NJ, Sanglard D, Gurr SJ. 2018. Worldwide emergence of resistance to antifungal drugs challenges human health and food security. *Science* **360:** 739-742.

Govrin EM, Levine A. 2000. The hypersensitive response facilitates plant infection by the necrotrophic pathogen *Botrytis cinerea*. *Current Biology* **10:** 751-757.

Gómez-Gómez L, Boller T. 2000. FLS2: an LRR receptor–like kinase involved in the perception of the bacterial elicitor flagellin in *Arabidopsis*. *Molecular Cell* **5**: 1003-1011.

Harper AL, Trick M, Higgins J, Fraser F, Clissold L, Wells R, Hattori C, Werner P, Bancroft I. 2012. Associative transcriptomics of traits in the polyploid crop species *Brassica napus*. *Nature Biotechnology* **30:** 798-802.

Havlickova L, He Z, Wang L, Langer S, Harper AL, Kaur H, Broadley MR, Gegas V, Bancroft I. 2018. Validation of an updated associative transcriptomics platform for the polyploid crop species *Brassica napus* by dissection of the genetic architecture of erucic acid and tocopherol isoform variation in seeds. *The Plant Journal* **93:** 181-192.

Hopkins MT, Lampi Y, Wang TW, Liu Z, Thompson JE. 2008. Eukaryotic translation initiation factor 5A is involved in pathogen-induced cell death and development of disease symptoms in Arabidopsis. *Plant Physiology* **148:** 479-489.

Hua K, Zhang J, Botella JR, Ma C, Kong F, Liu B, Zhu J-K. 2019. Perspectives on the application of genome-editing technologies in crop breeding. *Molecular Plant* **12:** 1047-1059.

Huang M, Liu X, Zhou Y, Summers RM, Zhang Z. 2019. BLINK: a package for the next level of genome-wide association studies with both individuals and markers in the millions. *Gigascience* **8:** giy154.

Hurni S, Scheuermann D, Krattinger SG, Kessel B, Wicker T, Herren G, Fitze MN, Breen J, Presterl T, Ouzunova M. 2015. The maize disease resistance gene *Htn1* against northern corn leaf blight encodes a wall-associated receptor-like kinase. *Proceedings of the National Academy of Sciences* **112:** 8780-8785.

Jia Y, McAdams SA, Bryan GT, Hershey HP, Valent B. 2000. Direct interaction of resistance gene and avirulence gene products confers rice blast resistance. *The EMBO Journal* **19:** 4004-4014.

Jones A. 2000. Does the plant mitochondrion integrate cellular stress and regulate programmed cell death? *Trends in Plant Science* **5:** 225-230.

Kemen E, Jones, JDG. 2012. Obligate biotroph parasitism: can we link genomes to lifestyles? *Trends in Plant Science* **17:** 448-457.

Kotchoni SO, Gachomo EW. 2006. The reactive oxygen species network pathways: an essential prerequisite for perception of pathogen attack and the acquired disease resistance in plants. *Journal of Biosciences* **31:** 389-404.

Kotchoni SO, Kuhns C, Ditzer A, Kirch HH, Bartels D. 2006. Over-expression of different *aldehyde dehydrogenase* genes in *Arabidopsis thaliana* confers tolerance to abiotic stress and protects plants against lipid peroxidation and oxidative stress. *Plant, Cell and Environment* **29:** 1033-1048.

Kou Y, Wang S. 2010. Broad-spectrum and durability: understanding of quantitative disease resistance. *Current Opinion in Plant Biology* **13:** 181-185.

Kunze G, Zipfel C, Robatzek S, Niehaus K, Boller T, Felix G. 2004. The N terminus of bacterial elongation factor Tu elicits innate immunity in Arabidopsis plants. *The Plant Cell* **16:** 3496-3507.

Kurowska M, Goudin N, Nehme NT, Court M, Garin J, Fischer A, de Saint Basile G, Ménasché G. 2012. Terminal transport of lytic granules to the immune synapse is mediated by the kinesin-1/Slp3/Rab27a complex. *Blood* **119:** 3879-3889.

Lacombe S, Rougon-Cardoso A, Sherwood E, Peeters N, Dahlbeck D, van Esse HP, Smoker M, Rallapalli G, Thomma BP, Staskawicz B et al. 2010. Interfamily transfer of a plant pattern-recognition receptor confers broad-spectrum bacterial resistance. *Nature Biotechnology,* **28:** 365-369.

Laluk K, Mengiste T. 2010. Necrotroph attacks on plants: wanton destruction or covert extortion? *The Arabidopsis Book* **8:** e0136

Levine A, Tenhaken R, Dixon R, Lamb C. 1994. H_2O_2 from the oxidative burst orchestrates the plant hypersensitive disease resistance response. *Cell* **79:** 583-593.

Lipka AE, Tian F, Wang Q, Peiffer J, Li M, Bradbury PJ, Gore MA, Buckler ES, Zhang Z. 2012. GAPIT: genome association and prediction integrated tool. *Bioinformatics* **28:** 2397-2399.

Liu X, Huang M, Fan B, Buckler ES, Zhang Z. 2016. Iterative usage of fixed and random effect models for powerful and efficient genome-wide association studies. *PLoS Genetics* **12:** e1005767.

Lloyd SR, Schoonbeek H-J, Trick M, Zipfel C, Ridout CJ. 2014. Methods to study PAMP-triggered immunity in *Brassica* species, *Molecular Plant-Microbe Interactions* **27:** 286-295.

Lorang JM, Sweat TA, Wolpert TJ. 2007. Plant disease susceptibility conferred by a “resistance” gene. *Proceedings of the National Academy of Sciences* **104:** 14861-14866.

Macioszek VK, Lawrence CB, Kononowicz AK. 2018. Infection cycle of *Alternaria brassicicola* on *Brassica oleracea* leaves under growth room conditions. *Plant Pathology* **67:** 1088-1096.

McCombe CL, Greenwood JR, Solomon PS, Williams SJ. 2022. Molecular plant immunity against biotrophic, hemibiotrophic, and necrotrophic fungi. *Essays in Biochemistry* **66:** 581-593.

McDowell JM, Woffenden BJ. 2003. Plant disease resistance genes: recent insights and potential applications. *Trends in Biotechnology* **21:** 178-183.

Miya A, Albert P, Shinya T, Desaki Y, Ichimura K, Shirasu K, Narusaka Y, Kawakami N, Kaku H, Shibuya N. 2007. CERK1, a LysM receptor kinase, is essential for chitin elicitor signaling in *Arabidopsis*. *Proceedings of the National Academy of Sciences* **104:** 19613-19618.

Moore JW, Herrera-Foessel S, Lan C, Schnippenkoetter W, Ayliffe M, Huerta-Espino J, Lillemo M, Viccars L, Milne R, Periyannan, S. 2015. A recently evolved hexose transporter variant confers resistance to multiple pathogens in wheat. *Nature Genetics* **47:** 1494-1498.

Nawrath C, Heck S, Parinthawong N, Métraux J-P. 2002. EDS5, an essential component of salicylic acid–dependent signaling for disease resistance in Arabidopsis, is a member of the MATE transporter family. *The Plant Cell* **14:** 275-286.

Nelson R, Wiesner-Hanks T, Wisser R, Balint-Kurti P. 2018. Navigating complexity to breed disease-resistant crops. *Nature Reviews Genetics* **19:** 21-33.

Ngou BPM, Ahn H-K, Ding P, Jones JDG. 2021. Mutual potentiation of plant immunity by cell-surface and intracellular receptors. *Nature* **592:** 110-115.

Nichols B. 2022. 'A pipeline for GEM And GWAS automation', *GitHub* URL https://github.com/bsnichols/GAGA.

Ogbomo H, Timm-McCann M, Barnes T, Xiang RF, Jamil K, Ganguly A, Stack D, Huston SM, Li SS, Colarusso P. 2018. Granule-dependent NK cell killing of cryptococcus requires kinesin to reposition the cytolytic machinery for directed cytotoxicity. *Cell Reports* **24:** 3017-3032.

Parinthawong N, Cottier S, Buchala A, Nawrath C, Métraux J-P. 2015. Localization and expression of EDS5H a homologue of the SA transporter EDS5. *BMC Plant Biology* **15:** 135.

Plaisier SB, Taschereau R, Wong JA, Graeber TG. 2010. Rank–rank hypergeometric overlap: identification of statistically significant overlap between gene-expression signatures. *Nucleic Acids Research* **38:** e169.

Roux F, Voisin D, Badet T, Balagué C, Barlet X, Huard-Chauveau C, Roby D, Raffaele S. 2014. Resistance to phytopathogens *e tutti quanti*: placing plant quantitative disease resistance on the map. *Molecular Plant Pathology* **15:** pp. 427-432.

Roy J, Shaikh TM, del Río Mendoza L, Hosain S, Chapara V, Rahman M. 2021. Genome-wide association mapping and genomic prediction for adult stage sclerotinia stem rot resistance in *Brassica napus* (L) under field environments. *Scientific Reports* **11:** 21773.

Samira R, Kimball JA, Samayoa LF, Holland JB, Jamann TM, Brown PJ, Stacey G, Balint-Kurti PJ. 2020. Genome-wide association analysis of the strength of the MAMP-elicited defense response and resistance to target leaf spot in sorghum. *Scientific Reports* **10:** 20817.

Sang Y, Macho AP. 2017. Analysis of PAMP-Triggered ROS Burst in Plant Immunity. In: Shan L, He P, eds. *Plant Pattern Recognition Receptors. Methods in Molecular Biology.* New York, USA: Humana Press, 143–153.

Schoonbeek H-J, Del Sorbo G, De Waard MA. 2001. The ABC transporter BcatrB affects the sensitivity of *Botrytis cinerea* to the phytoalexin resveratrol and the fungicide fenpiclonil. *Molecular Plant-Microbe Interactions* **14:** 562-571.

Schoonbeek H-J, Wang HH, Stefanato FL, Craze M, Bowden S, Wallington E, Zipfel C, Ridout CJ. 2015. Arabidopsis EF-Tu receptor enhances bacterial disease resistance in transgenic wheat. *New Phytologist* **206:** 606-613.

Schweizer P, Stein N. 2011. Large-scale data integration reveals colocalization of gene functional groups with meta-QTL for multiple disease resistance in barley. *Molecular Plant-Microbe Interactions* **24:** 1492-1501.

Schwessinger B, Bahar O, Thomas N, Holton N, Nekrasov V, Ruan D, Canlas PE, Daudi A, Petzold CJ, Singan VR. 2015. Transgenic expression of the dicotyledonous pattern recognition receptor EFR in rice leads to ligand-dependent activation of defense responses *PLoS Pathogens* **11:** e1004809.

Song J-M, Guan Z, Hu J, Guo C, Yang Z, Wang S, Liu D, Wang B, Lu S, Zhou R. 2020. Eight high-quality genomes reveal pan-genome architecture and ecotype differentiation of *Brassica napus*. *Nature Plants* **6:** 34-45.

Stefanato FL, Abou-Mansour E, Buchala A, Kretschmer M, Mosbach A, Hahn M, Bochet CG, Métraux JP, Schoonbeek H-J. 2009. The ABC

transporter BcatrB from *Botrytis cinerea* exports camalexin and is a virulence factor on *Arabidopsis thaliana*. *The Plant Journal* **58:** 499-510.

Storey JD. 2011. False Discovery Rate. In: Lovric M, eds. *International Encyclopedia of Statistical Science.* Heidelberg, Berlin, Germany: Springer, 504-508.

Stotz HU, Mitrousia GK, de Wit PJGM, Fitt BDL. 2014. Effector-triggered defence against apoplastic fungal pathogens. *Trends in Plant Science* **19:** 491-500.

Su Q, Rong W, Zhang Z. 2022. The pathogen-induced MATE gene *TaPIMA1* is required for defense responses to *Rhizoctonia cerealis* in wheat. *International Journal of Molecular Sciences* **23:** 3377.

Takanashi K, Shitan N, Yazaki K. 2014. The multidrug and toxic compound extrusion (MATE) family in plants. *Plant Biotechnology* **31:** 417-430.

Tiedemann AV. 1997. Evidence for a primary role of active oxygen species in induction of host cell death during infection of bean leaves with *Botrytis cinerea*. *Physiological and Molecular Plant Pathology* **50:** 151-166.

Vetter MM, Kronholm I, He F, Häweker H, Reymond M, Bergelson J, Robatzek S, de Meaux J. 2012. Flagellin perception varies quantitatively in *Arabidopsis thaliana* and its relatives. *Molecular Biology and Evolution* **29:** 1655-1667.

Vleeshouwers VGAA, van Dooijeweert W, Govers F, Kamoun S, Colon LT. 2000. The hypersensitive response is associated with host and nonhost resistance to *Phytophthora infestans*. *Planta* **210:** 853-864.

Wang J, Zhang Z. 2021. GAPIT Version 3: boosting power and accuracy for genomic association and prediction. *Genomics, Proteomics and Bioinformatics* **19:** 629-640.

Williams B, Kabbage M, Kim H-J, Britt R, Dickman MB. 2011. Tipping the balance: *Sclerotinia sclerotiorum* secreted oxalic acid suppresses host defenses by manipulating the host redox environment. *PLoS Pathogens* **7:** e1002107.

Wisser RJ, Sun Q, Hulbert SH, Kresovich S, Nelson RJ. 2005. Identification and characterization of regions of the rice genome associated with broad-spectrum, quantitative disease resistance. *Genetics* **169:** 2277-2293.

Yuan M, Ngou BPM, Ding P, Xin X-F. 2021. PTI-ETI crosstalk: an integrative view of plant immunity. *Current Opinion in Plant Biology* **62:** 102030.

Zeise K, Tiedemann AV. 2001. Morphological and physiological differentiation among vegetative compatibility groups of *Verticillium dahliae* in relation to *V. longisporum*. *Journal of Phytopathology* **149:** 469-475.

Zheng X. 2018. *Verticillium longisporum on oilseed rape (Brassica napus L.): differential roles of salicylic acid, seed transmission and plant colonization in greenhouse and field conditions.* PhD Thesis, Niedersächsische Staats-und Universitätsbibliothek Göttingen, Germany.

Zheng X, Koopmann B, von Tiedemann A. 2019. Role of salicylic acid and components of the phenylpropanoid pathway in basal and cultivar-related resistance of oilseed rape (*Brassica napus*) to *Verticillium longisporum*. *Plants* 8: 491.

Supporting information

Fig. S1 Comparisons between chitin-, flg22- and elf18-induced ROS responses for the phenotypes and associated gene expression markers (GEMs).

Fig. S2 Query coverage in *Brassica napus* reference genotypes and gene expression in *B. napus* population for region on chromosome C08 homoeologous to the region on A09 associated with resistance to *Verticillium longisporum.*

Table S1: Mean, normalized phenotype data for resistance to pathogens (*Alternaria brassicicola, Botrytis cinerea, Pyrenopeziza brassicae* and *Verticillium longisporum*) and ROS response induced by PAMPS (chitin, flg22, and elf18).

Table S2: Full list of single-nucleotide polymorphism (SNP) markers and significance levels from genome-wide association (GWA) analyses for resistance to pathogens (*Alternaria brassicicola, Botrytis cinerea, Pyrenopeziza brassicae* and *Verticillium longisporum*) and ROS response induced by PAMPS (chitin, flg22, and elf18).

Table S3: Full list of gene expression markers (GEMs) and significance levels from GEM analyses for resistance to pathogens (*Alternaria brassicicola, Botrytis cinerea, Pyrenopeziza brassicae* and *Verticillium longisporum*) and ROS response induced by PAMPS (chitin, flg22, and elf18).

Table S4: 184 gene expression markers (GEMs) associated with chitin-induced ROS compared with GEMs associated with resistance to pathogens (*Alternaria brassicicola, Botrytis cinerea, Pyrenopeziza brassicae* and *Verticillium longisporum*) and ROS response induced by flg22, and elf18. Lists correspond to Venn diagrams in Fig. 2.

Table S5: Enrichment analyses to determine if the number of gene expression markers (GEMs) shared between different lists is greater than the number of GEMs that would be expected by chance (e.g., lists of quantitative disease resistance (QDR) GEMs for two fungal pathogens).

Table S6: Shared gene expression markers (GEMs) associated with resistance to different pathogens (*Alternaria brassicicola, Botrytis cinerea, Pyrenopeziza brassicae* and *Verticillium longisporum*). Lists correspond to matrices and Venn diagrams in Fig. 3.

Table S7: List of genes in linkage disequilibrium with the top marker for *Verticillium longisporum* resistance from genome wide association (GWA) analysis on chromosome A09, the homoeologous region on C08, and their query coverage in *Brassica napus* reference genotypes.